Discrete spectral incoherent solitons in nonlinear media with noninstantaneous response

Claire Michel, Bertrand Kibler, Antonio Picozzi

Discrete spectral incoherent solitons in nonlinear media with noninstantaneous response

Claire Michel, Bertrand Kibler, and Antonio Picozzi

Laboratoire Interdisciplinaire Carnot de Bourgogne, UMR 5029 CNRS-Université de Bourgogne, 9 Avenuc A. Savary, F-21078 Dijon, France

(Received 1 October 2010; published 9 February 2011)

We show theoretically that nonlinear optical media characterized by a finite response time may support the existence of discrete spectral incoherent solitons. The structure of the soliton consists of three incoherent spectral bands that propagate in frequency space toward the low-frequency components in a discrete fashion and with a constant velocity. Discrete spectral incoherent solitons do not exhibit a confinement in the space-time domain, but exclusively in the frequency domain. The kinetic theory describes in detail all the essential properties of discrete spectral incoherent solitons: A quantitative agreement has been obtained between simulations of the kinetic equation and the nonlinear Schrödinger equation. Discrete spectral incoherent solitons may be supported in both the normal dispersion regime or the anomalous dispersion regime. These incoherent structures find their origin in the causality condition inherent to the nonlinear response function of the material. Considering the concrete example of the Raman effect, we show that discrete incoherent solitons may be spontaneously generated through the process of supercontinuum generation in photonic crystal fibers.

DOI: 10.1103/PhysRevA.83.023806 PACS number(s): 42.65.Tg, 42.65.Sf, 42.81.Dp

I. INTRODUCTION

The coherence properties of partially coherent optical waves propagating in nonlinear media have been studied since the advent of nonlinear optics in the 1960s. However, it is only recently that the dynamics of incoherent nonlinear optical waves has received renewed interest. The main motive for this renewal of interest is essentially due to the first experimental demonstration of incoherent solitons in both noninstantaneous [1,2] and instantaneous [3] response nonlinear media. The notable simplicity of experiments performed in photorefractive media has allowed for a fruitful investigation of the dynamics of incoherent nonlinear waves [4], as illustrated by several important achievements, such as, e.g., the modulational instability [5,6] or the bump-on-tail instability [7] of incoherent optical fields or the demonstration of incoherent dark solitons [8]. Quite remarkably, the existence of incoherent optical solitons has also been investigated theoretically [9] and has been demonstrated experimentally [10] in *discrete nonlinear media*. For a review we refer the reader to Ref. [11]. In some respects, these "random phase lattice solitons" generalize to the incoherent domain several key properties inherent to discrete solitons [12].

Different theories have been developed to provide a description of incoherent solitons in slowly responding nonlinear media [4]. The most established methods are the mutual coherence function approach [13], the self-consistent multimode theory [14], the coherent density method [15], and the Wigner transform approach [6]. These four methods are, in fact, equivalent [16] and the choice of the most suitable representation depends on the nature of the physical problem to be investigated. In particular, it is the self-consistent multimode theory [14] which has proven convenient to demonstrate the existence of discrete incoherent solitons in optical lattices [9].

More recently, an incoherent optical soliton of a fundamentally different nature has been identified in optical fibers by exploiting the stimulated Raman-scattering effect [17]. This incoherent structure has been called a "spectral incoherent soliton" because the optical field does not exhibit a confinement in the spatiotemporal domain, but exclusively in the frequency domain (also see Ref. [18]). More precisely, because the optical field exhibits fluctuations that are statistically stationary in time, the soliton behavior only manifests in the spectral domain. The analysis has revealed that the kinetic equation that describes spectral incoherent solitons has a rather simple structure. The same type of kinetic equation was, in fact, derived in the context of plasma physics to study weak Langmuir turbulence or stimulated Compton scattering [19–22].

The spectral incoherent soliton finds its origin in the property of causality of the nonlinear response function $\chi(t)$. Indeed, as a result of the causality condition the real and the imaginary parts of the Fourier transform of the response function $\widetilde{\chi}(\omega) = \widetilde{\chi}_{\rm r}(\omega) + i\,\widetilde{\chi}_{\rm i}(\omega)$ are known to be related by the Kramers-Krönig relations [23]. The imaginary part $\widetilde{\chi}_{\rm i}(\omega)$ plays the role of the "gain spectrum" for the field, which is responsible for an energy transfer from the high- to the low-frequency components of the incoherent field. After a transient, the averaged spectrum of the incoherent field self-organizes in the form of a spectral soliton, which propagates without distortion in frequency space toward the low-frequency components [17,21,22]. We note that, although our analysis may be applied to a variety of noninstantaneous Kerr nonlinearities characterized by the response function $\chi(t)$ (such as, e.g., the Maxwell-Debye model [24]), in the following we discuss spectral incoherent solitons within the framework of the concrete example of the Raman effect.

Our aim in this article is to show that spectral incoherent solitons may exhibit a discrete behavior. We show that, under certain conditions, the spectral incoherent soliton may become unstable and thus relaxes during the propagation toward its discrete counterpart. The discrete spectral incoherent soliton (DSIS) is essentially characterized by three *incoherent* spectral bands, whose frequencies refer to the central frequency ω_0 and the corresponding Stokes and anti-Stokes components with frequencies $\omega_j = \omega_0 \pm \omega_R$, ω_R being the Raman resonant frequency. As a result of the Raman effect, a new Stokes component is generated in the front of the soliton, which

becomes in turn the central band and finally the anti-Stokes band in the trailing edge of the soliton: a new (incoherent) spectral band grows up by absorbing the previously generated spectral band, until it is absorbed in turn by the newly generated band. In this way the DSIS propagates in frequency space toward the low-frequency components in a discrete fashion.

We show that all the essential properties of DSISs are described in detail by the corresponding kinetic equation that governs the evolution of the averaged spectrum of the field. In particular, a quantitative agreement has been obtained between the simulations of the kinetic equation and the nonlinear Schrödinger (NLS) equation, without using adjustable parameters. The kinetic approach also reveals that DSISs are supported in both the normal dispersion regime or the anomalous dispersion regime. Furthermore, we compare the DSIS solutions obtained numerically with an analytical soliton solution of the *discretezed* kinetic equation originally derived in Ref. [25], which models the DSIS frequency bands as coupled Dirac δ functions in frequency space (δ-peak model). The analysis reveals that, when injected as an initial condition into the kinetic equation, the analytical soliton solution rapidly relaxes during the propagation toward the DSIS solution. This property reveals the incoherent nature of DSIS. It also distinguishes the DSIS from the cascaded Raman soliton solutions reported in Refs. [26] or their recent generalizations [27], which involve several phase-locked Raman lines. Since these Raman solitons are inherently coherent localized structures, they are of a nature fundamentally different than that of the DSIS.

The DSIS may find applications in any optical system in which the noninstantaneous response of the nonlinearity cannot be neglected. In particular, the DSIS may emerge in the process of supercontinuum (SC) generation in photonic crystal fibers (PCF). SC generation is known to be characterized by a dramatic spectral broadening of the optical field during its propagation [28]. The interpretation of the mechanisms underlying SC generation, although generally well understood, constitutes a difficult problem due to the multitude of nonlinear effects involved. We note in this respect that a kinetic description of SC generation has recently been formulated [29,30]. We shall see that DSISs can be spontaneously generated through the process of SC generation in its highly nonlinear and quasi-continuous-wave regime.

II. EMERGENCE OF DSIS THROUGH SC GENERATION

In this section we show that DSIS-like structures may be spontaneously generated *via* the Raman effect in the process of SC generation in silica PCFs. For this purpose, we consider the generalized NLS equation, which is known to provide an accurate description of the propagation of an optical field in a PCF [28,31],

$$-i\frac{\partial\psi(z,t)}{\partial z}=\sum_{j\geqslant 2}^{m}\frac{i^j\beta_j}{j!}\frac{\partial^j\psi(z,t)}{\partial t^j}+\gamma\left(1+i\tau_s\frac{\partial}{\partial t}\right)\psi(z,t)\times\int_{-\infty}^{+\infty}R(t')|\psi(z,t-t')|^2dt', \quad (1)$$

where γ refers to the nonlinear coefficient and $R(t)=(1-f_R)\delta(t)+f_Rh_R(t)$ to the usual nonlinear response function of silica fibers, which accounts for both the instantaneous Kerr effect and the noninstantaneous Raman response function $h_R(t)$ [31]. It is important to include higher-order dispersion effects into the model Eq. (1) in order to describe broadband optical wave propagation. The higher-order time derivatives in Eq. (1) originate in a Taylor's expansion series of the dispersion curve of the PCF around the carrier angular-frequency ω_0 [28]. The corresponding dispersion relation of Eq. (1) then reads

$$k(\omega)=\sum_{j\geqslant 2}^{m}\frac{\beta_j\omega^j}{j!}. \quad (2)$$

Equation (1) also describes the self-steepening effect through the so-called optical shock term, i.e., the term proportional to $\tau_s\partial/\partial t$, with the shock time $\tau_s=1/\omega_0$. This time derivative term accounts for the dispersion of the nonlinearity [31]. We refer the reader to Refs. [28,31] for a detailed discussion of the different terms that appear in Eq. (1).

In recent works we have studied theoretically the highly nonlinear regime of SC generation in a PCF whose dispersion curve exhibits two zero-dispersion frequencies [29,30]. In this incoherent regime, rapid temporal fluctuations of the field prevent the formation of robust coherent structures, so that solitons do not play any significant role in the process of spectral broadening inherent to SC generation. We report in Fig. 1(a) a typical evolution of the spectrum of the field obtained by integrating numerically the NLS Eq. (1), with the dispersion curve, $k''(\omega)=\partial^2k(\omega)/\partial\omega^2$, reported in Fig. 1(b). The initial condition is a high-power (1 kW) continuous wave, in which a small amplitude noise has been superposed to initiate the modulational instability process. Indeed, the carrier frequency of the wave $\nu_0=282$ THz ($\lambda_0=1064$ nm) lies in the anomalous dispersion regime of the PCF; i.e., it is located between the two zero-dispersion wavelengths. The dispersion and nonlinear properties of the considered PCF are similar to those used in the experiment reported in Ref. [30].

Before analyzing the simulation reported in Fig. 1, let us briefly comment on the particularity and the possible future advantages of the SC configuration considered here. Indeed, in this configuration, the wavelength bands generated toward the midinfrared will allow for a long wavelength extension of standard cw-pumped supercontinuum. These sources have already been considered as practical solutions for high spectral power and spatially coherent sources. As a consequence, the SC regime considered here may open new applications by using low-cost and compact supercontinuum sources consisting of a nanosecond microchip pump laser and a single mode fiber (see the experiment of Ref. [30]). Obviously, the Raman-based SC extension requires good fiber transparency in the infrared, a property that can be also achieved with nonsilica glasses, such as, e.g., ZBLAN, tellurite, or chalcogenide fibers.

We may note in Fig. 1(a) that the spectrum of the field essentially splits into two components: a broad central part whose evolution is analyzed in Refs. [29,30] and a low-frequency branch that moves away from the central part of the spectrum. This low-frequency branch rapidly evolves toward a DSIS, which propagates with a constant velocity toward the low-frequency components. We remark that the discrete motion of the DSIS in frequency space is clearly apparent. The existence of the DSIS structure is exclusively

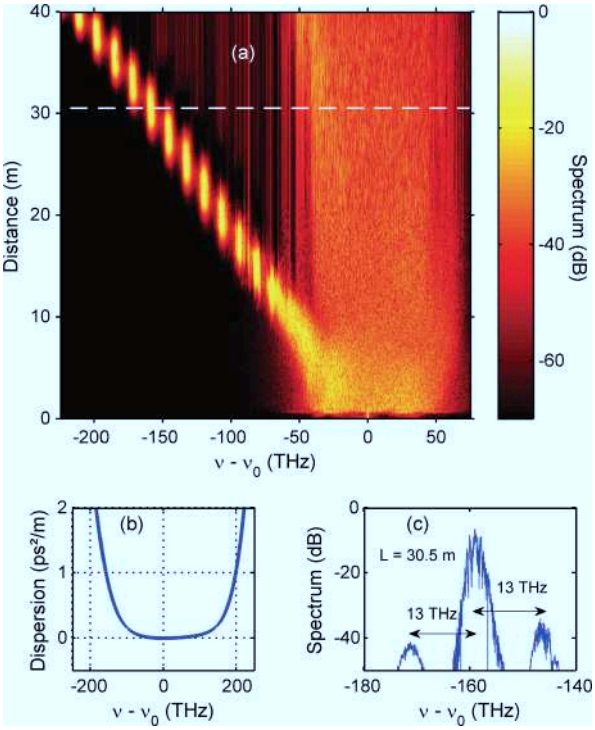

FIG. 1. (Color online) Spontaneous generation of the DSIS through SC generation. (a) Evolution of the spectrum of the optical field $|\tilde{\psi}|^2(z,\omega)$ (in dB scale) obtained by solving numerically the generalized NLS Eq. (1) for a PCF whose dispersion profile $k''(\omega) = \partial^2 k(\omega)/\partial\omega^2$ is reported in panel (b). A DSIS moves away from the central part of the spectrum: it propagates toward the low-frequency components in a discrete fashion and with a constant velocity. (c) Spectral profile of the optical field at the propagation length $z = 30.5$ m, showing that the frequency distance between adjacent bands corresponds to the Raman resonant frequency, $\omega_R/2\pi \simeq 13$ THz. The frequency $\nu_0 = \omega_0/2\pi$ is the carrier frequency of the initial cw field.

due to the stimulated Raman effect; i.e., numerical simulations performed without the Raman effect ($f_R = 0$) do not lead to the formation of the low-frequency branch and the DSISs are no longer generated. This is corroborated by the fact that the frequency distance between adjacent discrete bands precisely corresponds to the Raman resonant frequency ($\omega_R/2\pi \sim 13.2$ THz), as illustrated in Fig. 1(c), which reports the spectrum of the field at the propagation distance $z = 30.5$ m. We also remark in Fig. 1(c) that each individual discrete band is not coherent: the spectrum exhibits pronounced intensity fluctuations, thus indicating that the spectral components are not correlated with each other, a feature that will be confirmed later in this article. Despite such underlying incoherent structure, the low-frequency branch of the spectrum exhibits as a whole a regular discrete propagation toward the low-frequency components. Our aim in this article is to uncover the nature and the properties of these DSIS structures.

III. REDUCED NLS MODEL

We have seen in the previous section that the emergence of the DSIS is exclusively due to the Raman effect. In order to understand the nature of these incoherent structures, in the following we only retain the ingredients responsible for their generation. We thus focus our analysis to the study of a reduced NLS equation that solely takes into account the noninstantaneous response of the nonlinearity. We underline that this reduced NLS equation is quite general; i.e., it governs the evolution of an optical field $\psi(z,t)$ that propagates in a Kerr medium characterized by the nonlinear response function $\chi(t)$:

$$i\,\partial_z\psi = -\beta\,\partial_{tt}\psi + \gamma\,\psi\int_{-\infty}^{+\infty}\chi(\theta)\,|\psi|^2(z,t-\theta)\,d\theta. \quad (3)$$

In this equation the dispersion relation (2) has been truncated to the second order, $k(\omega) = \beta\omega^2$, where we have defined $\beta = \beta_2/2$. Although the theory may be applied to a large variety of response functions $\chi(t)$, we consider in the following the concrete and useful example of a damped harmonic oscillator response,

$$\chi(t) = H(t)\,\frac{\tau_1^2+\tau_2^2}{\tau_2\tau_1^2}\,\exp(-t/\tau_1)\,\sin(t/\tau_2). \quad (4)$$

This response function has been normalized in such a way that $\int\chi(t)dt = 1$. The presence of the Heaviside function $H(t)$ guarantees the causality condition of the response function, $\chi(t) = 0$ for $t < 0$. Note that in the limit $\tau_2 \gg \tau_1$, the sinus factor becomes irrelevant and the response function (4) recovers the purely exponential response involved in the Maxwell-Debye model equation [24], where τ_1 represents the response time of the material.

According to the linear response theory, the causality condition imposes restrictions on the Fourier transform of the response function

$$\tilde{\chi}(\omega) = \int_{-\infty}^{+\infty}\chi(t)\exp(-i\omega t)\,dt.$$

Because of the causality of $\chi(t)$, the function $\tilde{\chi}(\omega)$ is analytic in the lower half-plane $\mathrm{Im}(\omega) < 0$, so that the real and imaginary parts of $\tilde{\chi}(\omega) = \tilde{\chi}_\mathrm{r}(\omega) + i\,\tilde{\chi}_\mathrm{i}(\omega)$ turn out to be related by the Kramers-Krönig relations, $\tilde{\chi}_\mathrm{r}(\omega) = -\frac{1}{\pi}\mathcal{P}\int\frac{\tilde{\chi}_\mathrm{i}(\omega')}{\omega'-\omega}\,d\omega'$ and $\tilde{\chi}_\mathrm{i}(\omega) = \frac{1}{\pi}\mathcal{P}\int\frac{\tilde{\chi}_\mathrm{r}(\omega')}{\omega'-\omega}\,d\omega'$, where $\mathcal{P}$ denotes the principal Cauchy value [23]. We recall that $\tilde{\chi}_\mathrm{r}(\omega)$ is an even function, while $\tilde{\chi}_\mathrm{i}(\omega)$ is an odd function. The imaginary part $\tilde{\chi}_\mathrm{i}(\omega)$ is known to play the role of a "gain spectrum" for the optical field: the low-frequency components are amplified to the detriment of the high-frequency components [see, e.g., Fig. 2(a)]. We thus denote this gain curve by

$$g(\omega) = \tilde{\chi}_\mathrm{i}(\omega).$$

The resonant frequency ω_R denotes the maximum gain frequency of $g(\omega)$. We also remark that the causality condition of $\chi(t)$ breaks the Hamiltonian structure of the NLS Eq. (3), so that it only conserves the total power of the field

$$N = \int_{-\infty}^{+\infty}|\psi|^2\,dt. \quad (5)$$

The evolution of the random field $\psi(z,t)$ is characterized by two characteristic lengths, the nonlinear length $L_\mathrm{nl} = 1/(\gamma P)$ and the linear dispersion length $L_d = t_c^2/\beta$, where t_c is the coherence time of the field and $P = \langle|\psi|^2\rangle$ is the average power of the field. In the following we consider the weakly

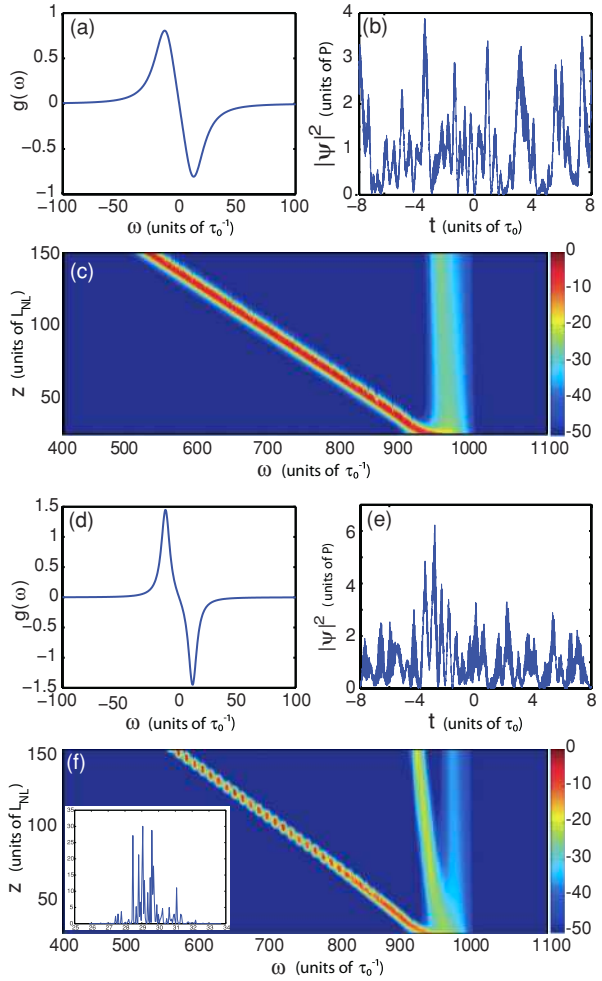

FIG. 2. (Color online) Influence of the gain spectrum $g(\omega)$ on the dynamics of spectral incoherent solitons. Gain spectra $g(\omega)$ for $\tau_1/\tau_2 = 1$ (a) and $\tau_1/\tau_2 = 2.6$ (d). Evolutions of the spectra of the field, $|\tilde{\psi}|^2(z,\omega)$ (in dB scale), obtained by solving numerically the NLS Eq. (3) for $\tau_1/\tau_2 = 1$ (c) and $\tau_1/\tau_2 = 2.6$ (f). The inset in panel (f) represents the spectrum of the field at $z_0 = 88L_{\rm nl}$. Temporal intensity profile $|\psi|^2(z_0,t)$ for $\tau_1/\tau_2 = 1$ (b) and $\tau_1/\tau_2 = 2.6$ (e) at $z_0 = 88L_{\rm nl}$, showing that the optical field is not localized in the time domain (the random wave exhibits a stationary statistics). Note that the dots in the DSIS in panel (f) are separated by ω_R in frequency space ($\tau_0 = 0.44$ ps, $\beta > 0$).

nonlinear (or highly incoherent) regime of interaction,

$$\rho = \frac{L_d}{L_{\rm nl}} \ll 1, \tag{6}$$

where the rapid temporal fluctuations of the field make linear effects dominant with respect to nonlinear effects. In this weakly nonlinear regime no coherent soliton solutions (e.g., Raman self-frequency-shift solitons) are generated [32].

For convenience, we present our results in normalized units, in which the field amplitude is measured in units of the square root of the average power P, the propagation length is measured in units of $L_{\rm nl}$, and the time is measured in units of $\tau_0 = (|\beta|L_{\rm nl})^{1/2}$. The variables can be recovered in real units through the transformations $t \to t\tau_0$, $z \to zL_{\rm nl}$, and $\psi \to \psi\sqrt{P}$.

A. Influence of the shape of the response function

A physical insight into DSISs may be obtained by a qualitative analysis of the shape of the response function $\chi(t)$ and the corresponding gain spectrum $g(\omega)$. We report in Fig. 2 two examples of gain spectra $g(\omega)$ that correspond to different ratios of the response times, $\tau_1/\tau_2 = 1$ [panel (a)] and $\tau_1/\tau_2 = 32/12.2 \simeq 2.6$ [panel (d)]. The latter case [panel (d)] is of particular interest since it corresponds to the example of the Raman response function in silica optical fibers, i.e., $\tau_1 = 32$ fs and $\tau_2 = 12.2$ fs [31]. We report in Figs. 2(c) and 2(f) the corresponding evolutions of the optical spectra obtained by integrating numerically the NLS Eq. (3). The initial condition is an incoherent wave characterized by a Gaussian spectrum with random spectral phases. It is superposed on a background of small noise of averaged intensity $\varepsilon = 10^{-5}$. The spectral components are δ-correlated in frequency space, so that the initial wave exhibits fluctuations that are statistically stationary in time. The background noise is important in order to sustain a steady soliton propagation, otherwise the soliton undergoes a slow adiabatic reshaping so as to adapt its shape to the local value of the noise background. The spectral width of the initial Gaussian spectrum has been chosen of the same order as ω_R, i.e., of the same order as the maximum gain frequency of $g(\omega)$. In this way the initial spectrum "feels" the whole spectral gain curve $g(\omega)$.

As illustrated in Fig. 2(c), the spectrum of the wave splits into two components during the propagation: a continuous spectral incoherent soliton emerges from the initial condition, while the remaining energy is characterized by a small-amplitude field, which essentially evolves linearly as a radiationlike part. This soliton behavior refers to the continuous spectral incoherent soliton investigated in the framework of the NLS Eq. (3) in the previous work [17]. Conversely, as the ratio τ_1/τ_2 increases, we see in Fig. 2(f) that the continuous spectral incoherent soliton is unstable and relaxes at $z \sim 60\ L_{\rm nl}$ toward a discrete soliton behavior. The DSIS is subsequently conserved for very long propagation distances, as remarkably illustrated in Fig. 2(f).

The fact that a continuous spectral incoherent soliton may become discrete during its evolution may easily be interpreted through a qualitative analysis of the gain curve $g(\omega)$. Indeed, a comparison of Figs. 2(a) and 2(d) clearly shows that the gain curve becomes narrower and more peaked as the ratio τ_1/τ_2 is increased, i.e., as the resonant frequency ω_R gets much larger than the spectral bandwidth of the gain curve, $\omega_R \gg \Delta\omega$. As a result, the red-shift of the wave spectrum becomes discrete, because the leading edge of the low-frequency tail of the spectrum exhibits a much higher gain as compared to the mean gain of the whole front of the spectrum. The remarkable result is that the global spectral red-shift exhibits a genuine discrete solitonlike behavior: The DSIS propagates with a constant velocity in frequency space for arbitrary long distances, without emitting any apparent radiation.

Let us finally underline that the optical field associated with the DSIS exhibits a stationary statistics. This is illustrated in Figs. 2(b) and 2(e), which report typical temporal intensity profiles associated with the continuous and the discrete solitons considered in Figs. 2(c) and 2(f). We note that the optical field exhibits temporal fluctuations at any time; i.e., the fluctuations are statistically stationary in time. This means

that, as for continuous spectral incoherent solitons [17], the soliton behavior of the DSIS does not manifest into the temporal domain, but exclusively in the spectral domain. Note that stationary statistics for the random field implies that its frequency components are δ correlated (see Sec. IV), a feature which is corroborated by the pronounced intensity fluctuations in the wave spectrum [see the inset in Fig. 2(f)].

B. Influence of the background noise intensity

The relative intensity of the background noise with respect to the average power of the wave plays an important role in the dynamics of DSISs. Indeed, the *continuous* spectral incoherent soliton is known to become narrower (i.e., of higher amplitude) as the intensity of the background noise decreases. This property is apparent in the analytical soliton solution found in Ref. [22] and is subsequently generalized in Ref. [33]. Accordingly, we may expect a transition from the continuous spectral incoherent soliton to a DSIS as the relative intensity of the background noise is decreased: as the spectral soliton becomes narrower than ω_R, the leading edge of the tail of the spectrum will be preferentially amplified, thus leading to the formation of a DSIS.

We verified the existence of the transition from the continuous to the discrete spectral incoherent soliton by the numerical simulations of the NLS Eq. (3). The results are reported in Fig. 3, which illustrates the evolution of the spectrum of the field during the propagation for different values of the background noise intensity, keeping constant the average power of the field. As expected, a continuous spectral soliton is generated for a relatively high background noise intensity, while a transition to a DSIS is observed as the noise intensity decreases. Also note that the velocity of the spectral soliton decreases as the intensity of the backgound noise decreases.

Note that the statistical properties of the background noise do not affect the dynamics of the DSIS. We performed numerical simulations with a background noise whose *amplitude* fluctuations were characterized by either a Gaussian statistics or an exponential statistics. No apparent differences were observed in the DSIS properties, despite the different variances of intensity fluctuations ($\langle I^2 \rangle$) that characterize the Gaussian and the exponential statistics. We remark that this result is corroborated by the kinetic wave theory exposed in Sec. IV, since the kinetic equation (8) does not take into account the statistical properties of the background noise.

C. Normal and anomalous dispersion

It is important to underline that DSISs may be supported in both the normal dispersion regime or the anomalous dispersion regime. This is illustrated in Fig. 4, which reports the evolution of the spectrum of the wave with exactly the same parameters and the same initial condition as in Fig. 3(b), except that now propagation takes place in the anomalous dispersion regime [$\beta < 0$ in Eq. (3)]. A comparison of Figs. 4 and 3(b) clearly shows that the evolution of the spectrum is not sensitive to the sign of the dispersion coefficient. This is due to the fact that wave propagation takes place in the highly incoherent (i.e., weakly nonlinear) regime, as discussed above through the criterion (6). This aspect becomes apparent in the derivation

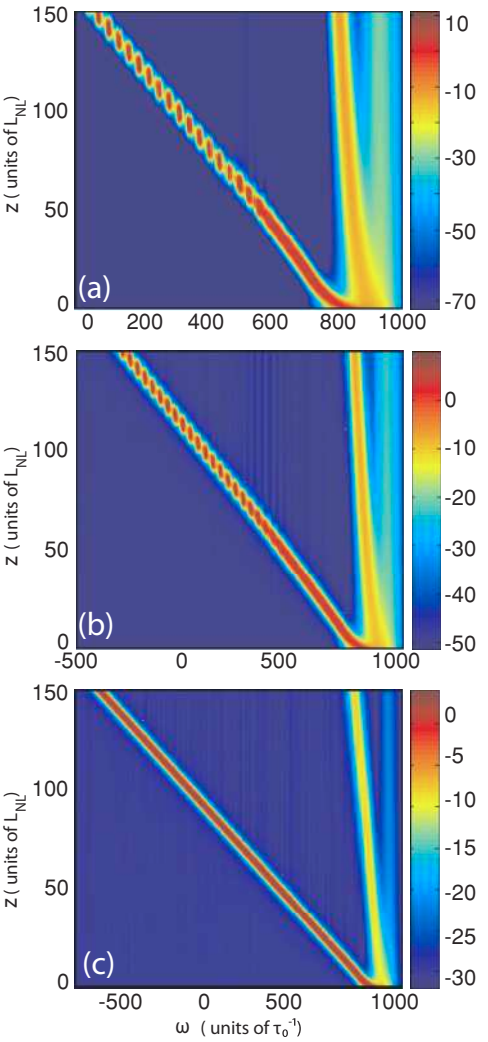

FIG. 3. (Color online) Transition from discrete to continuous spectral incoherent soliton. Evolution of the nonaveraged spectrum of the optical field, $|\tilde{\psi}|^2(z,\omega)$ (in dB scale), obtained by integrating numerically the NLS Eq. (3) for three different values of the noise background: $\varepsilon = 10^{-7}$ (a), $\varepsilon = 10^{-5}$ (b), and $\varepsilon = 10^{-3}$ (c). We considered the ratio $\tau_1/\tau_2 = 2.6$ in the gain spectrum $g(\omega)$, and $\tau_0 = 0.44$ ps ($\beta > 0$). Note the quantitative agreement with the corresponding simulations of the kinetic Eq. (8), without using adjustable parameters (see Fig. 5).

of the kinetic equation reported in Sec. IV, since the kinetic Eq. (8) does not depend on linear dispersion effects.

Note however that the existence of the DSIS requires the combined contributions of linear dispersion effects and nonlinear effects. Indeed, in the absence of linear dispersion the spectrum would be highly deformed, thus preventing the formation of a soliton structure, while in the absence of nonlinearity the spectrum would not evolve at all.

IV. KINETIC APPROACH

A. Kinetic equation

The numerical simulations of the NLS Eq. (3) discussed in Sec. III correspond to a single realization of the initial random

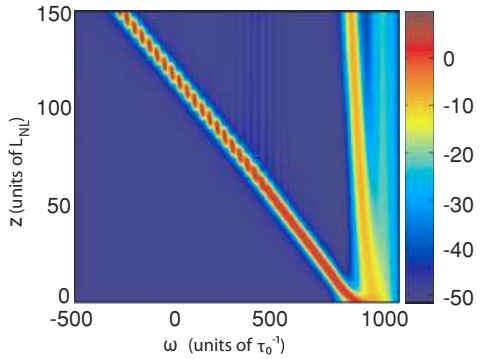

FIG. 4. (Color online) Same as in Fig. 3(b), but in the *anomalous* dispersion regime, $\beta < 0$. DSISs are also supported with anomalous dispersion and, more generally, the evolution of the wave is not sensitive to the sign of the dispersion coefficient. The dots in the soliton trajectories are separated by the resonant frequency ω_R.

noise of the field $\psi(z = 0,t)$. In this way, the corresponding evolutions of the spectra $|\tilde{\psi}|^2(z,\omega)$ reported above refer to a nonaveraged random function. Obviously, such a *stochastic* function cannot describe a genuine soliton evolution. In order to reveal the underlying *deterministic* soliton behavior, one has to resort to a statistical description of the incoherent field, which is based on an average over the realizations ($\langle\cdot\rangle$) of the random field. More precisely, we are looking for the kinetic equation describing the evolution of the averaged spectrum of the field. We refer the reader to Ref. [33] for technical details regarding the derivation of the kinetic equation associated with the delayed NLS Eq. (3). Here we briefly recall the main steps of the derivation.

The starting point is to follow the usual procedure to derive an equation describing the evolution of the autocorrelation function $C(z,t_1,t_2) = \langle\psi(z,t_1)\psi^*(z,t_2)\rangle$. Because of the nonlinear character of the NLS Eq. (3), the evolution of the second-order moment of the field $C(z,t_1,t_2)$ depends on the fourth-order moment. In turn, the equation for the fourth-order moment depends on the sixth-order moment, thus leading to an infinite hierarchy of moment equations. This makes the equations impossible to solve unless some way can be found to truncate the hierarchy. This refers to the fundamental problem of achieving a closure of the infinite hierarchy of the moment equations [34]. A simple way to achieve the closure of the hierarchy is to assume that the field has Gaussian statistics. This approximation is justified in the weakly nonlinear regime considered here, $\rho = L_d/L_{\rm nl} \ll 1$. Note that in this weakly nonlinear regime the statistics do not need to be Gaussian initially: linear dispersive effects dominate the interaction and bring the system to a state of Gaussian statistics. In practice, the closure of the hierarchy is achieved by exploiting the property of factorizability of moments of Gaussian fields. The corresponding equation for the autocorrelation function is quite complicated in the general case [33]. However, a considerable simplification occurs here because we deal with an optical field that exhibits a stationary statistics. Then it proves convenient to introduce the change of variables $t = (t_1 + t_2)/2$ and $\tau = t_1 - t_2$, which leads to the following closed equation for the second-order moment $B(z,\tau) = C(z,t + \tau/2,t - \tau/2) = \langle\psi(z,t + \tau/2)\psi^*(z,t - \tau/2)\rangle$ [17,33]:

$$i\,\partial_z B(z,\tau) = \gamma \int_0^{+\infty} \chi(t)[B(t)B(\tau - t) - B^*(t)B(\tau + t)]\,dt, \tag{7}$$

where $B(t)$ stands for $B(z,t)$ in the integrand. According to the Wiener-Kintchine theorem [35], the averaged spectrum of the field is given by the Fourier transform of the autocorrelation function, $n(z,\omega) = \int B(z,\omega)\,\exp(-i\omega t)\,dt$,

$$\partial_z n(z,\omega) = \frac{\gamma}{\pi}\, n(z,\omega) \int_{-\infty}^{+\infty} g(\omega - \omega')\, n(z,\omega')\, d\omega', \tag{8}$$

where $n(z,\omega)$ refers to the averaged spectrum of the field, $\langle\tilde{\psi}(z,\omega + \Omega/2)\tilde{\psi}^*(z,\omega - \Omega/2)\rangle = n(z,\omega)\delta(\Omega)$.

The kinetic Eq. (8) has been the subject of a detailed study in the context of plasma physics, in which it is usually referred to the weak Langmuir turbulence kinetic equation. For a review on this subject we refer the reader to Ref. [19]. We briefly summarize here the essential properties of the kinetic Eq. (8). First, this equation does not account for dispersion effects [Eq. (8) does not depend on β], although the role of dispersion in its derivation is essential in order to verify the criterion (6), $\rho \ll 1$. The fact that the dynamics of the DSIS does not depend on the sign of the dispersion coefficient has been verified by direct numerical simulations of the NLS Eq. (3) in Sec. III C. The kinetic Eq. (8) conserves the power of the field $N = \int n_\omega(z)\,d\omega$. Moreover, the kinetic Eq. (8) is a formally reversible equation; i.e., it is invariant under the transformation $(z,\omega) \to (-z,-\omega)$ [36]. This is consistent with the fact that Eq. (8) conserves another important quantity, namely, the nonequilibrium entropy of the field, $S = \int \ln[n_\omega(z)]\,d\omega$. Accordingly, Eq. (8) does not exhibit an H theorem of entropy growth, which means that it is does not describe the process of optical wave thermalization. This aspect is discussed in more detail in Sec. V. Finally, the fact that Eq. (8) may exhibit solitary-wave solutions may be anticipated by remarking that, as a result of the convolution product, the spectral gain curve $g(\omega)$ amplifies the front of the spectrum at the expense of its trailing edge, thus leading to a global red-shift of the spectrum.

B. Agreement between kinetic and NLS simulations

A continuous spectral incoherent soliton solution of the kinetic Eq. (8) can be generated in the presence of a background noise of constant intensity, $n_\omega \to \varepsilon = n_\infty > 0$, as $|\omega| \to \pm\infty$ [19,21,22]. This is illustrated in Fig. 5, which shows the evolution of the averaged spectrum $n(z,\omega)$ obtained by integrating numerically the kinetic Eq. (8). As discussed above through the numerical simulations of the NLS Eq. (3) in Fig. 3, a transition from the continuous to the discrete spectral incoherent soliton is observed as the intensity of the background noise, ε, is decreased. We report in Figs. 5(a)–5(c) a series of numerical simulations corresponding to three different values of the background noise intensity. In order to test the validity of the kinetic Eq. (8), these numerical simulations have been realized with the same parameters and the same initial conditions as those of the NLS Eq. (3) reported in Fig. 3. We underline that an excellent agreement has been obtained between them, *without using any adjustable*

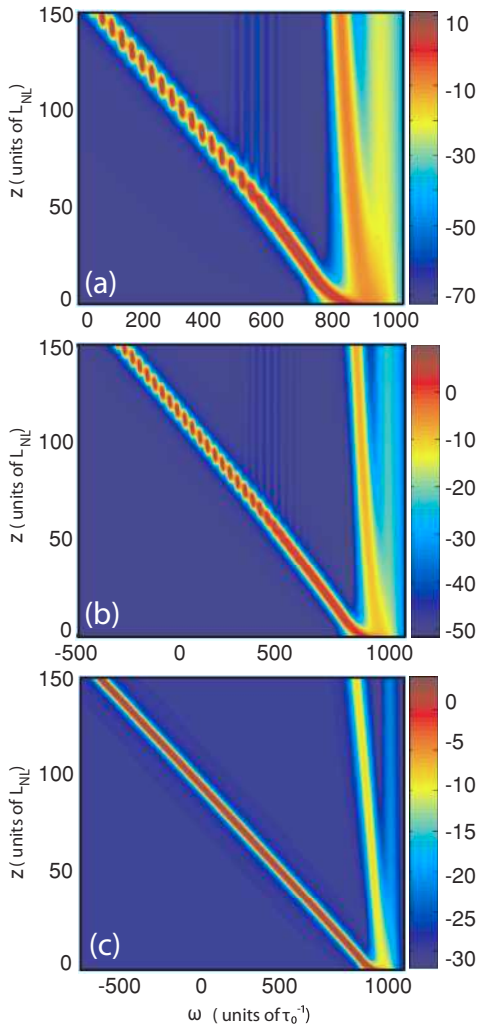

FIG. 5. (Color online) Evolution of the averaged spectrum of the optical field, $n(z,\omega)$ (in dB scale), obtained by integrating numerically the kinetic Eq. (8) for three different values of the noise background: $\varepsilon = 10^{-7}$ (a), $\varepsilon = 10^{-5}$ (b), and $\varepsilon = 10^{-3}$ (c). We considered the ratio $\tau_1/\tau_2 = 2.6$ in the gain spectrum $g(\omega)$. Note the quantitative agreement with the corresponding simulations of the NLS Eq. (3), without using adjustable parameters (see Fig. 3).

parameter. We also note that such a good agreement has been obtained with a reasonable value of the small parameter $\rho \sim 0.02$.

Let us remark that continuous spectral incoherent soliton solutions of the kinetic Eq. (8) may be derived in the limit where the bandwidth of the gain curve is much larger than the soliton spectral width [20]. Indeed, in this limit one may approximate the gain spectrum as $g(\omega) \propto \omega$, which readily gives a Gaussian-shaped soliton solution to Eq. (8). It is interesting to notice that discrete spectral incoherent solitons cannot be described with this approximation of the gain curve. This becomes apparent by referring back to the discussion of the influence of the shape of the gain spectrum on the dynamics of spectral incoherent solitons. Indeed, we show in Sec. III A that a DSIS can be generated provided that the (Raman) resonant frequency is much larger than the spectral bandwidth of the gain curve, $\omega_R \gg \Delta\omega$. This condition implies constraints on the shape of the gain spectrum that cannot be captured by a simple first-order expansion of $g(\omega)$.

C. Soliton solution of the discrete δ-peak model

If the limit where the spectral width of the optical field is much smaller than the resonant frequency ω_R [but still large enough to verify the criterion (6)], the wave spectrum may be expanded as a sum of equally spaced Dirac δ functions,

$$n(z,\omega) = \sum_m N_m(z)\,\delta(\omega - m\omega_R), \tag{9}$$

where N_m represents the amplitude of the m peak at the frequency $\omega = m\omega_R$. One may substitute the ansatz (9) into the kinetic Eq. (8), which gives the following *discrete nonlinear equation* [25]:

$$d_z N_m = \frac{\gamma g_0}{\pi} N_m(N_{m+1} - N_{m-1}), \tag{10}$$

where $g_0 = g(-\omega_R)$ is the value of maximum gain at $\omega = -\omega_R$. The nonlinear discrete structure of the kinetic Eq. (10) may easily be interpreted: the central band N_m is absorbed by the Stokes component N_{m-1}, while it is simultaneously amplified by the anti-Stokes component N_{m+1}. It is important to note that the discrete model (10) has been shown to be completely integrable by the inverse scattering method [37].

An analytical soliton solution to the discrete δ-peak model may be written in the following form [25],

$$N(vz + m\omega_R) = N_0\left(1 + \frac{a}{1 - b + b\cosh[q(vz + m\omega_R)]}\right), \tag{11}$$

where N_0 is the background noise intensity, q is the inverse characteristic width of the soliton, and v is the soliton velocity in frequency space, i.e., the coordinate of the maximum of the soliton decreases as $-vz/\omega_R$. The parameters are related by the following relations, $a(1-b) = b^2\sinh^2(q\omega_R)$ and $a = 2(1-b)[\cosh(q\omega_R) - 1]$ and the velocity is given by $v = \frac{2\gamma g_0 N_0}{\pi q}\sinh(q\omega_R)$, which gives $a = 4(1-b)[1 + (1-b)^2/b^2]$.

This analytical soliton solution has been put as an initial condition into the numerical simulations of the kinetic Eq. (8). The corresponding evolution of the spectrum $n_\omega(z)$ is reported in Fig. 6. For concreteness, we considered here the gain curve $g(\omega)$ corresponding to the Raman response function of silica optical fibers. We clearly see in Fig. 6 that the soliton solution (11) rapidly relaxes toward a DSIS solution of the continuous kinetic Eq. (8). A detailed analysis reveals that the background noise level N_0 in Eq. (11) gets amplified by the broad spectral gain $g(\omega)$ during the propagation, which merely explains why the soliton (11) relaxes toward a DSIS solution of Eq. (8).

In other terms, a prerequisite for the soliton (11) to be robust under the evolution of the continuous kinetic Eq. (8) is that the spectral width of the gain curve $\Delta\omega$ almost coincides with the tiny width of the δ peaks involved in the discretized model (10). If this condition is not verified, the underlying peaks of (11) inevitably exhibit a deformation, thus bringing the analytical soliton solution toward a DSIS solution of the

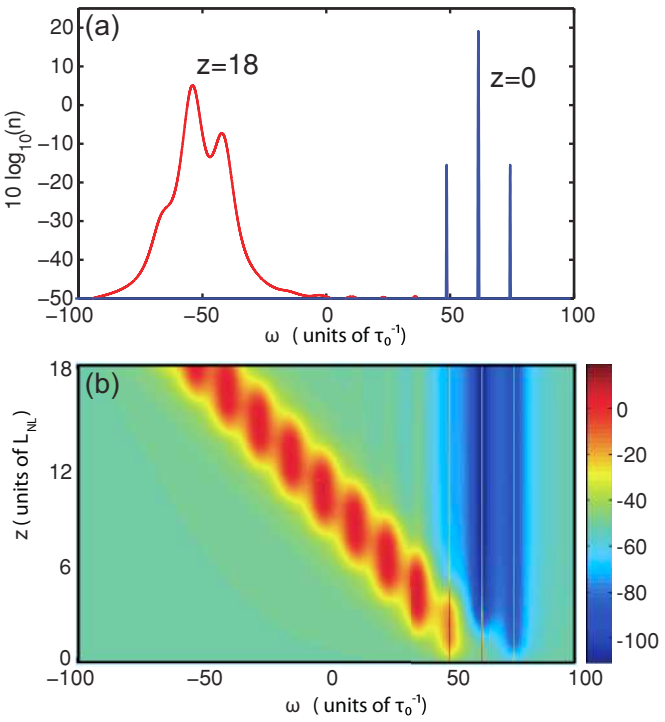

FIG. 6. (Color online) Spectral profiles at $z = 0$ and $z = 18$ (a), and corresponding evolution of the spectrum $n(z,\omega)$ (in dB scale) (b), obtained by solving numerically the kinetic Eq. (8) starting from the analytical soliton solution (11) at $z = 0$: the soliton solution relaxes toward a DSIS ($\tau_1/\tau_2 = 2.6, \tau_0 = 0.156$ ps).

continuous kinetic Eq. (8). Another important constraint of the soliton solution (11) is that the spectral width $\Delta\omega$ of the δ peaks should be large enough to verify the criterion (6), i.e., $\Delta\omega \gg \sqrt{\gamma P/\beta}$.

V. DISCUSSION

It is interesting to discuss the relevance of the DSIS from a more general perspective. Indeed, the study of the long-term evolution of an incoherent optical field is attracting a growing interest in the optics community (see, e.g., Ref. [38]). In particular, the thermalization [29,30,39] and the condensation [40] of optical waves have been studied in various circumstances and in various optical media characterized by different nonlinearities. Of particular interest is the process of optical wave condensation, which has been studied in conservative (Hamiltonian) systems [40], as well as in laser systems [41]. In complete analogy with the kinetics of a gas system, optical wave thermalization in conservative systems manifests itself by means of an irreversible evolution of the optical field toward the thermodynamic equilibrium state, i.e., the Rayleigh-Jeans spectrum. The wave turbulence (WT) theory [32,34,42] is known to provide a detailed description of this nonequilibrium thermalization process. In contrast with the WT kinetic equation, the Langmuir-like kinetic Eq. (8) describing the DSIS is formally reversible, a feature which is consistent with the fact that it conserves the nonequilibrium entropy. Actually, it is the causality property inherent to the nonlinear response function $\chi(t)$ which prevents the thermalization process from occurring. This becomes apparent by remarking that Eq. (3) is almost identical to the NLS equation governing wave propagation in a *nonlocal* nonlinear medium [4], provided one substitutes the response function with the nonlocal potential, $\chi(t) \to V(\mathbf{r})$ and $t \to \mathbf{r}$. However, nonlocal effects are not constrained by the causality condition. Instead of being causal, the function $V(\mathbf{r})$ is even, which is a consequence of the usual assumption of spatial homogeneity. Its Fourier transform $\widetilde{V}(\mathbf{k})$ is thus purely real; i.e., the gain spectrum vanishes identically, $g(\omega) = 0$. The kinetic Eq. (8) then reduces to the trivial equation $\partial_z n(z,\mathbf{k}) = 0$. This means that the kinetic description of a nonlocal interaction requires a second-order perturbation expansion in ρ, and the corresponding kinetic equation exhibits the usual H theorem of entropy growth describing the irreversible thermalization process. This comparison between nonlocal and noninstantaneous nonlinearities reveals that (in the first-order approximation in ρ) the causality property inherent to the response function $\chi(t)$ prevents the field from reaching thermal equilibrium. In other terms, the analysis reveals that *the DSIS constitutes a nonstationary and nonequilibrium stable state of the incoherent field*. In this respect, we note that, besides the nonequilibrium kinetic wave approach used here, the equilibrium properties of a random nonlinear wave may be studied on the basis of statistical mechanics by computing appropriate partition functions, a feature that has been analyzed in various circumstances [43]. According to the previous discussion, these equilibrium statistical approaches are inherently unable to describe the nonequilibrium DSIS structures studied here.

Let us finally comment on the possible relevance of this work in the context of fiber optics communication systems. Indeed, in the wavelength division multiplexing technique, one deals with a random pulse sequence that propagates along different channels and that experiences a random energy exchange due to the Raman effect [44]. In particular, this problem was also studied in relation to random cascade models in developed turbulence [45]. It would be interesting to analyze the possible relevance of spectral incoherent solitons in these optical communication systems.

In summary, we have shown theoretically that optical nonlinearities characterized by a noninstantaneous response may support the existence of discrete incoherent soliton structures. The structure of the soliton consists of three incoherent spectral bands that propagate in frequency space with a constant velocity and in a discrete fashion. A kinetic approach to the problem revealed that the causality property inherent to the material response function is responsible for the existence of these incoherent structures. DSISs may be thus expected to arise in a large variety of nonlinear media whose finite response times cannot be neglected. We showed, in particular, that they may be spontaneously generated in the highly nonlinear regime of the process of SC generation in silica PCF. The experiment aimed at reporting the observation of DSISs through SC generation is in progress. We underline the quantitative agreement obtained in the simulations of the kinetic Eq. (8) and the NLS Eq. (3), without using any adjustable parameter (see Figs. 3 and 5). We finally note that, beyond optics, spectral incoherent solitons may find applications in many branches of nonlinear physics owing to the universality of the NLS equation.

[1] M. Mitchell, Z. Chen, M. F. Shih, and M. Segev, Phys. Rev. Lett. **77**, 490 (1996); M. Mitchell and M. Segev, Nature (London) **387**, 880 (1997).

[2] See, e.g., D. N. Christodoulides, T. H. Coskun, M. Mitchell, and M. Segev, Phys. Rev. Lett. **78**, 646 (1997); M. Mitchell, M. Segev, T. H. Coskun, D. N. Christodoulides, *ibid.* **79**, 4990 (1997); D. N. Christodoulides, T. H. Coskun, M. Mitchell, Z. Chen, and M. Segev, *ibid.* **80**, 5113 (1998); Z. Chen *et al.*, Science **280**, 889 (1998); O. Bang, D. Edmundson, and W. Krolikowski, Phys. Rev. Lett. **83**, 5479 (1999); N. N. Akhmediev and A. Ankiewicz, *ibid.* **83**, 4736 (1999); N. M. Litchinitser, W. Krolikowski, N. N. Akhmediev, and G. P. Agrawal, Phys. Rev. E **60**, 2377 (1999); M. Peccianti and G. Assanto, Opt. Lett. **26**, 1791 (2001); S. A. Ponomarenko and G. P. Agrawal, Phys. Rev. E **69**, 036604 (2004).

[3] A. Picozzi and M. Haelterman, Phys. Rev. Lett. **86**, 2010 (2001); A. Picozzi, C. Montes, and M. Haelterman, Phys. Rev. E **66**, 056605 (2002); A. Picozzi, M. Haelterman, S. Pitois, and G. Millot, Phys. Rev. Lett. **92**, 143906 (2004); A. Picozzi and P. Aschieri, Phys. Rev. E **72**, 046606 (2005); M. Wu, P. Krivosik, B. A. Kalinikos, and C. E. Patton, Phys. Rev. Lett. **96**, 227202 (2006); O. Cohen, H. Buljan, T. Schwartz, J. W. Fleischer, and M. Segev, Phys. Rev. E **73**, 015601 (2006); C. Rotschild *et al.*, Nat. Photonics **2**, 371 (2008).

[4] Y. S. Kivshar and G. P. Agrawal, *Optical Solitons: From Fibers to Photonic Crystals* (Academic Press, San Diego, 2003).

[5] See, e.g., M. Soljacic, M. Segev, T. Coskun, D. N. Christodoulides, and A. Vishwanath, Phys. Rev. Lett. **84**, 467 (2000); D. Kip *et al.*, Science **290**, 495 (2000); C. Anastassiou, M. Soljacic, M. Segev, E. D. Eugenieva, D. N. Christodoulides, D. Kip, Z. H. Musslimani, and J. P. Torres, Phys. Rev. Lett. **85**, 4888 (2000); J. P. Torres, C. Anastassiou, M. Segev, M. Soljacic, and D. N. Christodoulides, Phys. Rev. E **65**, 015601 (2001); H. Buljan, A. Siber, M. Soljacic, and M. Segev, *ibid.* **66**, 035601 (2002); L. Helczynski, M. Lisak, and D. Anderson, *ibid.* **67**, 026602 (2003); D. Anderson, L. Helczynski-Wolf, M. Lisak, and V. Semenov, *ibid.* **69**, 025601 (2004); K. Motzek *et al.*, Opt. Lett. **29**, 280 (2004); D. Anderson, L. Helczynski-Wolf, M. Lisak, and V. Semenov, Phys. Rev. E **70**, 026603 (2004); M. Jablan *et al.*, Opt. Express **15**, 4623 (2007); A. Sauter, S. Pitois, G. Millot, and A. Picozzi, Opt. Lett. **30**, 2143 (2005).

[6] B. Hall, M. Lisak, D. Anderson, R. Fedele, and V. E. Semenov, Phys. Rev. E **65**, 035602 (2002).

[7] D. V. Dylov and J. W. Fleischer, Phys. Rev. Lett. **100**, 103903 (2008); Phys. Rev. A **78**, 061804 (2008).

[8] See, e.g., D. N. Christodoulides, T. H. Coskun, M. Mitchell, Z. Chen, and M. Segev, Phys. Rev. Lett. **80**, 5113 (1998); Z. Chen *et al.*, Science **280**, 889 (1998).

[9] H. Buljan, O. Cohen, J. W. Fleischer, T. Schwartz, M. Segev, Z. H. Musslimani, N. K. Efremidis, and D. N. Christodoulides, Phys. Rev. Lett. **92**, 223901 (2004).

[10] O. Cohen *et al.*, Nature (London) **433**, 500 (2005).

[11] H. Buljan *et al.*, Stud. Appl. Math. **115**, 173 (2005).

[12] F. Lederer *et al.*, Phys. Rep. **463**, 1 (2008); D. N. Christodoulides *et al.*, Nature (London) **424**, 817 (2003).

[13] G. A. Pasmanik, Sov. Phys. JETP **39**, 234 (1974).

[14] M. Mitchell, M. Segev, T. H. Coskun, and D. N. Christodoulides, Phys. Rev. Lett. **79**, 4990 (1997).

[15] D. N. Christodoulides, T. H. Coskun, M. Mitchell, and M. Segev, Phys. Rev. Lett. **78**, 646 (1997).

[16] D. N. Christodoulides, E. D. Eugenieva, T. H. Coskun, M. Segev, and M. Mitchell, Phys. Rev. E **63**, 035601 (2001); M. Lisak, L. Helczynski, and D. Anderson, Opt. Commun. **220**, 321 (2003).

[17] A. Picozzi, S. Pitois, and G. Millot, Phys. Rev. Lett. **101**, 093901 (2008).

[18] A. V. Gorbach and D. V. Skryabin, Opt. Lett. **31**, 3309 (2009).

[19] S. L. Musher, A. M. Rubenchik, and V. E. Zakharov, Phys. Rep. **252**, 177 (1995).

[20] A. S. Kompaneets, Zh. Eksp. Teor. Fiz. **31**, 871 (1956); Sov. Phys. JETP. **4**, 730 (1957); A. A. Galeev, V. I. Karpman, and R. Z. Sagdeev, Dokl. Akad. Nauk SSSR **157**, 1088 (1964); A. A. Galeev, V. I. Karpman, and R. Z. Sagdeev, Dokl. Akad. Sov. Phys. Dokl. **9**, 681 (1965); H. Dreicer, Phys. Fluids **7**, 735 (1964); Ya. B. Zel'dovich and E. V. Levich, Zh. Eksp. Teor. Fiz. **55**, 2423 (1968); Sov. Phys. JETP. **28**, 1287 (1969); J. Peyraud, J. Phys. (Paris) **29**, 872 (1968); **29**, 88 (1968).

[21] Ya. B. Zel'dovich and R. A. Syunyaev, Sov. Phys. JETP **35**, 81 (1972); Ya. B. Zel'dovich, E. V. Levich, and R. A. Syunyaev, *ibid.* **35**, 733 (1972); V. E. Zakharov, S. L. Musher, and A. M. Rubenchik, *ibid.* **42**, 80 (1976); C. Montes, J. Peyraud, and M. Hénon, Phys. Fluids **22**, 176 (1979).

[22] C. Montes, Phys. Rev. A **20**, 1081 (1979).

[23] R. W. Boyd, *Nonlinear Optics* (Academic Press, San Diego, 2008).

[24] A. C. Newell and J. V. Moloney, *Nonlinear Optics* (Addison–Wesley, Reading, MA, 1992).

[25] V. E. Zakharov, S. L. Musher, and A. M. Rubenchik, JETP Lett. **19**, 151 (1974).

[26] A. E. Kaplan, Phys. Rev. Lett. **73**, 1243 (1994); A. E. Kaplan, P. L. Shkolnikov, and B. A. Akanaev, Opt. Lett. **19**, 445 (1994); A. E. Kaplan and P. L. Shkolnikov, J. Opt. Soc. Am. B **13**, 347 (1996); G. S. McDonald, Opt. Lett. **20**, 822 (1995).

[27] D. V. Skryabin, F. Biancalana, D. M. Bird, and F. Benabid, Phys. Rev. Lett. **93**, 143907 (2004); D. V. Skryabin and A. V. Yulin, Phys. Rev. E **74**, 046616 (2006); D. V. Skryabin, A. V. Yulin, and F. Biancalana, *ibid.* **73**, 045603 (2006); A. V. Gorbach and D. V. Skryabin, Opt. Express **16**, 4858 (2008).

[28] J. M. Dudley, G. Genty, and S. Coen, Rev. Mod. Phys. **78**, 1135 (2006).

[29] B. Barviau *et al.*, Opt. Lett. **33**, 2833 (2008); B. Barviau, B. Kibler, and A. Picozzi, Phys. Rev. A **79**, 063840 (2009).

[30] B. Barviau *et al.*, Opt. Express **17**, 7392 (2009).

[31] G. P. Agrawal, *Nonlinear Fiber Optics*, 4th ed. (Academic Press, San Diego, 2006).

[32] V. E. Zakharov, F. Dias, and A. Pushkarev, Phys. Rep. **398**, 1 (2004).

[33] J. Garnier and A. Picozzi, Phys. Rev. A **81**, 033831 (2010).

[34] K. Hasselmann, J. Fluid Mech. **12**, 481 (1962); **15**, 273 (1963); D. J. Benney and P. G. Saffman, Proc. R. Soc. London A **289**, 301 (1966); A. C. Newell, Rev. Geophys. **6**, 1 (1968); D. J. Benney and A. C. Newell, Stud. Appl. Math **48**, 29 (1969).

[35] L. Mandel and E. Wolf, *Optical Coherence and Quantum Optics* (Cambridge University Press, New York, 1995).

[36] Note that the requirement of the sign inversion in ω can be understood by analogy with kinetic gas theory, where time reversal needs the inversion of the momentum of the particles, $(t, \boldsymbol{p}) \rightarrow (-t, -\boldsymbol{p})$.

[37] S. V. Manakov, Sov. Phys. JETP **40**, 269 (1975).

[38] B. Barviau, S. Randoux, and P. Suret, Opt. Lett. **31**, 1696 (2006); A. Picozzi and M. Haelterman, Phys. Rev. Lett. **92**, 103901 (2004); A. Mussot *et al.*, Opt. Express **17**, 17010 (2009); L. Levi *et al.*, *ibid.* **16**, 7818 (2008); A. Fratalocchi, C. Conti, G. Ruocco, and S. Trillo, Phys. Rev. Lett. **101**, 044101 (2008); Y. Silberberg, Y. Silberberg, Y. Lahini, Y. Bromberg, E. Small, and R. Morandotti, *ibid.* **102**, 233904 (2009); K. Hammani *et al.*, Phys. Lett. A **374**, 3585 (2010).

[39] S. Pitois, S. Lagrange, H. R. Jauslin, and A. Picozzi, Phys. Rev. Lett. **97**, 033902 (2006); S. A. Babin, V. Karalekas, E. V. Podivilov, V. K. Mezentsev, P. Harper, J. D. Ania-Castanon, and S. K. Turitsyn, J. Opt. Soc. Am. B **24**, 1729 (2007); S. Babin *et al.*, Phys. Rev. A **77**, 033803 (2008); A. Picozzi, Opt. Express **15**, 9063 (2007); S. Lagrange, H. R. Jauslin, and A. Picozzi, Europhys. Lett. **79**, 64001 (2007); A. Picozzi, Opt. Express **16**, 17171 (2008); P. Suret, S. Randoux, H. R. Jauslin, and A. Picozzi, Phys. Rev. Lett. **104**, 054101 (2010); C. Michel *et al.*, Opt. Lett. **35**, 2367 (2010).

[40] S. Dyachenko *et al.*, Physica D **57**, 96 (1992); M. J. Davis, S. A. Morgan, and K. Burnett, Phys. Rev. Lett. **87**, 160402 (2001); C. Connaughton, C. Josserand, A. Picozzi, Y. Pomeau, and S. Rica, *ibid.* **95**, 263901 (2005); G. Düring, A. Picozzi, and S. Rica, Physica D **238**, 1524 (2009); A. Picozzi and S. Rica, Europhys. Lett. **84**, 34004 (2008); H. Salman and N. Berloff, Physica D **238**, 1482 (2009); U. Bortolozzo *et al.*, J. Opt. Soc. Am. B **26**, 2280 (2009).

[41] C. Conti, M. Leonetti, A. Fratalocchi, L. Angelani, and G. Ruocco, Phys. Rev. Lett. **101**, 143901 (2008); E. G. Turitsyna, G. Falkovich, V. K. Mezentsev, and S. K. Turitsyn, Phys. Rev. A **80**, 031804 (2009); R. Weill, B. Fischer, and O. Gat, Phys. Rev. Lett. **104**, 173901 (2010); R. Weill *et al.*, Opt. Express **18**, 16520 (2010).

[42] V. N. Tsytovich, *Nonlinear Effects in Plasma* (Plenum, New York, 1970); A. Hasegawa, *Plasma Instabilities and Nonlinear Effects* (Springer-Verlag, Berlin, 1975); V. E. Zakharov, V. S. L'vov, and G. Falkovich, *Kolmogorov Spectra of Turbulence I* (Springer, Berlin, 1992); S. Dyachenko *et al.*, Physica D **57**, 96 (1992); A. C. Newell, S. Nazarenko, and L. Biven, *ibid.* **152**, 520 (2001).

[43] See, e.g., R. Jordan, B. Turkington, and C. L. Zirbel, Physica D **137**, 353 (2000); K. Rasmussen, T. Cretegny, P. G. Kevrekidis, and N. Gronbech-Jensen, Phys. Rev. Lett. **84**, 3740 (2000); B. Rumpf and A. C. Newell, *ibid.* **87**, 054102 (2001); A. Eisner and B. Turkington, Physica D **213**, 85 (2006); B. Rumpf and A. C. Newell, *ibid.* **184**, 162 (2003); B. Rumpf, Phys. Rev. E **69**, 016618 (2004); Physica D **238**, 2067 (2009); A. Fratalocchi, C. Conti, G. Ruocco, and S. Trillo, Phys. Rev. Lett. **101**, 044101 (2008).

[44] A. R. Chraplyvy, Electron. Lett. **20**, 58 (1984); F. Forghieri, R. W. Tkach, and A. R. Chraplyvy, IEEE Photonics Technol. Lett. **7**, 101 (1995); D. N. Christodoulides and R. B. Jander, *ibid.* **8**, 1722 (1996); K. P. Ho, J. Lightwave Technol. **18**, 915 (2000); A. Peleg, Opt. Lett. **29**, 1980 (2004); H. Kim, S. B. Jun, and Y. C. Chung, IEEE Photonics Technol. Lett. **19**, 695 (2007); Y. Chung and A. Peleg, Phys. Rev. A **77**, 063835 (2008); Q. M. Nguyen and A. Peleg, Opt. Commun. **283**, 3500 (2010).

[45] A. Peleg, Phys. Lett. A **373**, 2734 (2009).